# Aharonov-Bohm Effect on Landau States in Annular Cylindrical Boxes

E. Ley-Koo[1*], G. Villa-Torres[1*], and D. Kouznetsov[2]

[1]*Instituto de Física-UNAM., Apartado Postal 20-364, 01000 México, D. F. México*

[2]*Mathematical Building, Box 87, University of Arizona, Tucson, AZ 85721, USA*

(Received September 24, 2001)

The Schrödinger equation for an electron inside an annular cylindrical box and in the presence of an axial uniform magnetic field is solved in two comparative situations: i) when the magnetic induction $\mathbf{B}_0 = \hat{k}B_0$ is the same in the central perforation and in the box, and ii) when its values in the perforation $\mathbf{B}_i = \hat{k}B_i$ and in the box $\mathbf{B}_0 = \hat{k}B_0$ are different. The Aharonov-Bohm effect on the Landau states of the confined electron is exhibited through the analysis of the dependence of the energy eigenvalues and eigenfunctions on the difference of the magnetic flux in the perforation as $B_i - B_0$ changes.

PACS. 03.65.–w – Quantum mechanics.
PACS. 03.65.Bz – Aharonov-Bohm effect.

## I. Introduction

This paper deals with the problem of an electron moving under the action of uniform magnetic fields combining the situations of the Landau problem [1-3] and of the Aharonov-Bohm (A-B) effect [4-6]. The first situation corresponds to a uniform magnetic induction at all points of space and to an electron allowed to be at any of those points. The Landau problem has been solved in both the linear gauge and the symmetric gauge, and the connections between the respective eigenstates have been exhibited in [3]. The second situation involves a uniform magnetic induction in a limited region of space from which the electron is excluded. Aharonov and Bohm predicted that the fringe pattern in an electron interference experiment should be shifted by altering the amount of magnetic flux passing between two beams, even though the beams themselves pass only through field-free regions [4]. The experiments performed by Chambers using magnetic whiskers confirmed this prediction [5]. The A-B effect on the bound states of an electron inside an annular cylindrical box was analyzed in [6].

The A-B effect on the Landau states of an electron inside an annular cylindrical box is investigated by comparing two new situations. In Sec. II, the same uniform magnetic induction $\mathbf{B}(0 \le \rho \le b; \varphi; z) = \hat{k}B_0$ is present in the central perforation $(0 \le \rho \le a)$ and in the box $(a \le \rho \le b)$. In Sec. III, the magnetic induction in the perforation $\mathbf{B}(0 \le \rho \le b; \varphi; z) = \hat{k}B_i$ is different from the one in the box $\mathbf{B}(a \le \rho \le b; \varphi; z) = \hat{k}B_0$. The analysis of both situations involves identifying the respective vector potentials in the perforation and in the box, constructing the Hamiltonians via the minimal-coupling prescription, and solving the corresponding Schrödinger equations. The box is assumed to be impenetrable, which translates into the boundary condition that the eigenfunctions must vanish at the positions of the walls of the box. Sec. IV presents numerical and graphical results illustrating the A-B effect through the changes of the energy eigenvalues and eigenfunction parameters as the magnetic flux difference in the perforation $(B_i - B_0)\pi a^2$ changes, including a discussion of these results. For completeness sake the explicit forms of the Kummer confluent hypergeometric functions are included in the Appendix.

## II. Landau states in an annular cylindrical box

This section presents the formulation and solution of the quantum problem of an electron, of mass $m_e$ and electric charge $-e$, confined inside an annular cylindrical box $(a \le \rho \le b; 0 \le \varphi \le 2\pi; 0 \le z \le L)$, and under the action of an axial uniform magnetic field,

$$\vec{B}(0 \le \rho \le b; \varphi; z) = \hat{k} B_0; \tag{1}$$

which has the same magnitude in both the perforation and the box. The associated magnetic vector potential is chosen as the one in the symmetric gauge,

$$\vec{A}(0 \le \rho \le b; \varphi; z) = \hat{\varphi}\frac{B_0 \rho}{2}; \tag{2}$$

congruent with the geometry of the box. The Hamiltonian for the system is constructed by using the minimal-coupling prescription [2],

$$H = \frac{(\vec{p} + \frac{e}{c}\vec{A})^2}{2m_e} = \frac{p_\rho^2}{2m_e} + \frac{(\frac{l_z}{\rho} + \frac{eB_0\rho}{2c})}{2m_e} + \frac{p_z^2}{2m_e}; \tag{3}$$

involving the radial $p_\rho$, azimuthal $l_z/\rho$, and axial $p_z$ components of the canonical momentum; $l_z$ is the canonical angular momentum. Then the corresponding time-independent Schrödinger equation becomes

$$\left\{ -\frac{\hbar^2}{2m_e}\frac{1}{\rho}\frac{\partial}{\partial\rho}\rho\frac{\partial}{\partial\rho} + \frac{\hat{l}_z^2}{2m_e\rho^2} + \frac{eB_0}{2m_e c}\hat{l}_z + \frac{e^2B_0^2}{8m_e c^2}\rho^2 - \frac{\hbar^2}{2m_e}\frac{\partial^2}{\partial z^2} \right\} \psi(\rho;\varphi;z) = E\psi(\rho;\varphi;z): \tag{4}$$

The three terms coming from the square of the binomial in Eq. (3) are identified as the rotational kinetic energy, the diamagnetic energy, and the harmonic oscillator potential energy with a frequency $\omega = eB_0/2m_e c$.

Equation (4) admits separable solutions

$$\psi(\rho;\varphi;z) = R(\rho)\Phi(\varphi)Z(z): \tag{5}$$

Each factor satisfies the respective ordinary differential equation in the longitudinal, azimuthal and radial coordinate:

$$-\frac{\hbar^2}{2m_e}\frac{d^2Z}{dz^2} = E^L Z; \tag{6}$$

$$-i\hbar\frac{d\Phi}{d\varphi} = m\hbar\Phi; \tag{7}$$

$$\left\{ -\frac{\hbar^2}{2m_e}\left[\frac{1}{\rho}\frac{d}{d\rho}\rho\frac{d}{d\rho} - \frac{m^2}{\rho^2}\right] + \frac{1}{2}m_e\omega^2\rho^2 + m\hbar\omega \right\} R = E^T R. \tag{8}$$

Here the longitudinal and transverse contributions to the energy add up to the total energy,

$$E^L + E^T = E. \tag{9}$$

The eigensolutions of Eq. (6) are determined by the boundary conditions that they must vanish at the lower $z = 0$ and upper $z = L$ walls of the box. Their explicit form is

$$Z_n(z) = \sqrt{\frac{2}{L}}\sin\frac{n\pi z}{L}, \quad n = 1, 2, 3, \ldots . \tag{10}$$

The corresponding longitudinal eigenenergy becomes

$$E_n^L = \frac{\hbar^2 n^2\pi^2}{2m_e L^2}. \tag{11}$$

Equation (7) is the eigenvalue equation for the $z$-component of the angular momentum, with eigensolutions

$$\Phi_m(\varphi) = \frac{e^{im\varphi}}{\sqrt{2\pi}} \tag{12}$$

and integer eigenvalues

$$m = 0, \pm 1, \pm 2, \ldots \tag{13}$$

arising from the periodicity condition $\Phi(\varphi + 2\pi) = \Phi(\varphi)$.

Apart from the diamagnetic energy term, Eq. (8) is identified as the radial Schrödinger equation for a two-dimensional isotropic harmonic oscillator. Its solutions are well-known; for the electron inside the annular cylindrical box they must vanish at the inner $\rho = a$ and outer $\rho = b$ walls. The general solution is

$$\begin{aligned} R(\rho) = \rho^{|m|} e^{-m_e\omega\rho^2/2\hbar} \Big\{ & C M\left(-\nu, |m| + 1, \frac{m_e\omega\rho^2}{\hbar}\right) \\ & + D U\left(-\nu, |m| + 1, \frac{m_e\omega\rho^2}{\hbar}\right) \Big\}, \end{aligned} \tag{14}$$

in terms of the confluent hypergeometric functions $M$ and $U$ [7], where the transverse eigenenergy contribution has the form

$$E_{sm}^T = \hbar\omega\,[2\nu_s + |m| + 1 + m]. \tag{15}$$

The radial boundary conditions become:

$$C M\left(-\nu, |m| + 1, \frac{m_e\omega a^2}{\hbar}\right) + D U\left(-\nu, |m| + 1, \frac{m_e\omega a^2}{\hbar}\right) = 0, \tag{16}$$

$$C M\left(-\kappa; |m|+1; \frac{m_e\omega b^2}{\hbar}\right) + D U\left(-\kappa; |m|+1; \frac{m_e\omega b^2}{\hbar}\right) = 0. \tag{17}$$

The value of the transverse eigenenergy parameter $\kappa$ is determined by the condition that the determinant of the two linear homogeneous algebraic Eqs. (16) and (17) in $C$ and $D$ vanishes,

$$\begin{aligned} &M\left(-\kappa; |m|+1; \frac{m_e\omega a^2}{\hbar}\right) U\left(-\kappa; |m|+1; \frac{m_e\omega b^2}{\hbar}\right) \\ &- U\left(-\kappa; |m|+1; \frac{m_e\omega a^2}{\hbar}\right) M\left(-\kappa; |m|+1; \frac{m_e\omega b^2}{\hbar}\right) = 0. \end{aligned} \tag{18}$$

For an electron confined in an annular cylindrical box with inner and outer radii $a$ and $b$, under the action of the uniform magnetic induction field defined by Eq. (1), and in an eigenstate with a chosen value of $m$, Eq. (13), the zeros of Eq. (18) for $\kappa_s$, $s = 1, 2, 3, \ldots$ determine the corresponding radial eigenfunctions $R_{sm}(\rho)$, Eq. (14), and transverse eigenenergies $E^T_{sm}$, Eq. (15). Such zeros are computed numerically using the appropriate representations of the functions $M$ and $U$ [7], Eqs. (A.1), (A.4) with $\alpha = -\kappa$ and $n = |m|$.

The normal Landau problem in which the electron may be at any point in the range $0 \le \rho < \infty$ corresponds to the particular case of $a = 0$ and $b = \infty$. By recalling that $U$ is singular at $\rho = 0$ its presence in Eq. (14) must be eliminated by taking $D = 0$. On the other hand, $M$ diverges as $\exp(m_e\omega\rho^2/\hbar)$ as $\rho \to \infty$, Eq. (A.5), and the only way to make Eq. (14) still useful is to take $\kappa$ as a non-negative integer $N$ for which $M$ becomes a polynomial of degree $2N$. Correspondingly, the Landau energy levels of Eq. (15) become the spectrum of odd integers in units $\hbar\omega$, each level being infinitely degenerate on account of the cancellation of the rotation and diamagnetic contributions $|m| + m$ for $m = -|m|$.

The zeros of $\kappa_s$ in Eq. (18) depend on the values of the other parameters of $M$ and $U$, namely $|m|$, $(m_e\omega a^2/\hbar)$, and $(m_e\omega b^2/\hbar)$ and in general are not integers. The dimensionless parameter $m_e\omega b^2/\hbar$ can be rewritten in terms of the magnetic induction field as $B_0\pi b^2/(hc/e)$, which can be identified as the magnetic flux in the circular cross-section of radius $b$ expressed in the fluxon unit, $hc/e = 4.135 \times 10^{-7}$ gauss-cm$^2$. The result of the confinement of the electron inside the annular cylindrical box is to remove the infinite degeneracy of the normal Landau energy levels described in the previous paragraph. Explicit numerical illustrations of these results are shown in Sec. IV.

## III. Aharonov-bohm effect on the landau states in an annular cylindrical box

In this section we analyze the changes in the eigenenergies and eigenfunctions of the Landau states when the magnetic induction field has a value in the perforation different form its value in the box. Let the respective values be

$$\vec{B}(0 \le \rho \le a; \varphi; z) = \hat{k} B_i \tag{19}$$

and

$$\vec{B}(a \le \rho \le b; \varphi; z) = \hat{k} B_0. \tag{20}$$

The corresponding magnetic vector potential is

$$\begin{aligned} \vec{A}(0 \le \rho \le a; \varphi; z) &= \hat{\varphi}\frac{B_i \rho}{2}; \\ \vec{A}(a \le \rho \le b; \varphi; z) &= \hat{\varphi}\left[\frac{B_0 \rho}{2} + \frac{(B_i - B_0)a^2}{2\rho}\right]. \end{aligned} \tag{21}$$

This potential is continuous at the boundary $\rho = a$, and its curl reproduces the magnetic induction fields in the perforation and in the box. The Hamiltonian for the electron in the box becomes

$$H = \frac{p_\rho^2}{2m_e} + \frac{\left[\frac{l_z}{\rho} + \frac{e(B_i - B_0)a^2}{2c\rho} + \frac{eB_0\rho}{2c}\right]^2}{2m_e} + \frac{p_z^2}{2m_e}. \tag{22}$$

The difference of the magnetic induction in the perforation, Eq. (19), compared to the one in the box, Eq. (20), is translated into the difference of the magnetic vector potential of Eq. (21) compared to that of Eq. (2) and correspondingly to the difference between the Hamiltonian of Eq. (22) compared to that of Eq. (3). The latter consists in the replacement

$$l_z \to l_z + \frac{e(B_i - B_0)a^2}{2c} \tag{23}$$

in going from Eq. (3) to Eq. (22), in the terms inversely proportional to the radial coordinate $\rho$. Then the new time-independent Schrodinger equation is

$$\begin{aligned} \Bigg\{ &-\frac{\hbar^2}{2m_e}\frac{1}{\rho}\frac{\partial}{\partial\rho}\rho\frac{\partial}{\partial\rho} + \frac{\left[\hat{l}_z + \frac{e(B_i - B_0)a^2}{2c}\right]^2}{2m_e\rho^2} + \frac{eB_0}{m_e c}\left[\hat{l}_z + \frac{e(B_i - B_0)a^2}{2c}\right] \\ &+ \frac{e^2 B_0^2}{8m_e c^2}\rho^2 - \frac{\hbar^2}{2m_e}\frac{\partial^2}{\partial z^2}\Bigg\}\Psi(\rho; \varphi; z) = E\,\Psi(\rho; \varphi; z); \end{aligned} \tag{24}$$

instead of Eq. (4). It also admits separable solutions of the same type of Eq. (5), with the same longitudinal and azimuthal eigenfunctions and eigenvalues of Eqs. (10)-(13) satisfying the corresponding differential Eqs. (6) and (7). The radial differential equation becomes

$$\left\{-\frac{\hbar^2}{2m_e}\left[\frac{1}{\rho}\frac{d}{d\rho}\rho\frac{d}{d\rho} - \frac{(m+\mu)^2}{\rho^2}\right] + \frac{1}{2}m_e\omega^2\rho^2 + \hbar\omega(m+\mu)\right\}R = E^T R; \tag{25}$$

where

$$\mu = \frac{e(B_i - B_0)a^2}{2\hbar c} = \frac{(B_i - B_0)\pi a^2}{(hc/e)} \tag{26}$$

is the change in the magnetic flux in the perforation in the fluxon unit when the magnetic induction changes from its value of Eq. (1) to that of Eq. (19). The difference in going from the radial Eq. (8) to that of Eq. (25) is the replacement

$$m \to m + \mu; \tag{27}$$

which follows from that of Eq. (22).

The solutions of the radial Eq. (25) are of the same type as those of Eq. (8) with the replacement of Eq. (27). Their explicit forms are

$$R_{sm}(\rho;\mu) = \rho^{|m+\mu|} e^{-m_e\omega\rho^2/2\hbar} \left\{ C M\left(-\nu; |m+\mu|+1; \frac{m_e\omega\rho^2}{\hbar}\right) + D U\left(-\nu; |m+\mu|+1; \frac{m_e\omega\rho^2}{\hbar}\right) \right\} \quad (28)$$

instead of Eq. (14), with the new transverse eigenenergy

$$E^T_{sm}(\mu) = \hbar\omega[2\nu_s + |m+\mu| + 1 + m + \mu]; \quad (29)$$

instead of Eq. (15), and the ratio of the $C$ and $D$ coefficients and the parameter $\nu$ being determined by

$$\frac{C}{D} = -\frac{U(-\nu; |m+\mu|+1; \frac{m_e\omega a^2}{\hbar})}{M(-\nu; |m+\mu|+1; \frac{m_e\omega a^2}{\hbar})} = -\frac{U(-\nu; |m+\mu|+1; \frac{m_e\omega b^2}{\hbar})}{M(-\nu; |m+\mu|+1; \frac{m_e\omega b^2}{\hbar})} \quad (30)$$

instead of Eqs. (16)-(18). Of course, for the case in which $B_i = B_0$ the value of $\mu$ vanishes, Eq. (26), and the results of Sec. II are recovered. For the general case of interest here $B_i \neq B_0$, and the A-B effect on the Landau states in the annular cylindrical box is associated with the $\mu$ dependence of the radial eigenfunctions, Eq. (28), and the transverse eigenenergies, Eq. (29), determined by the values of $\nu_s$ solutions of Eq. (30), with $s = 1, 2, 3, \ldots$. Here the Eq. (A.3) for $U$ must be used for non integer values of $\mu$. Numerically computed values of $\nu_s$ and $E^T_{sm}(\mu)$ for different chosen values of $\mu$ are presented in the following section.

## IV. Numerical results and discussion

This section contains some numerical and graphical results illustrating the confinement effect of the annular box on the Landau states, and the A-B effect on the same states, from the analysis in Section II and III, respectively. For the first one, the zeros of Eq. (18) in $\nu$ are based on the logarithmic form of the $U$ function, Eq. (A.4). For the second one, Eq. (30) requires the use of the form of $U$ of Eq. (A.3) for non-integer values of $\mu$. Table I and Fig. 1 illustrate the confinement effect, and Table II and Fig. 2 the A-B effect on the Landau states, as explained and discussed next.

Table I presents the transverse energy eigenvalues $E^T_{sm}$ for the Landau states with $s$ = 1, 2, and 3, and $m = 0, \pm 1, \pm 2, \ldots$ obtained from Eqs. (15) and (18), for the electron confined in boxes with $b = 2a$, 5$a$ and 10$a$, in different magnetic induction fields producing magnetic fluxes of 1 and 15 fluxons in the circular cross sections of radius $b$. The values of $\nu_s$ from the numerical solution of Eq. (18), when doubled and increased by one unit, give the energy eigenvalues for the zero and negative $m$ states; for the positive $m$ states the further addition of $2m$ is required.

The confinement effect of the box on the electron Landau states is obviously manifested by the departure of the energy levels from the equally spaced and infinitely degenerate $(2N+1)\hbar\omega$ spectra with integer values of $N$. The data in Table I indicate that such an effect is dominant

TABLE I. Radial s and angular momentum m quantum numbers and transverse energy eigenvalues $E^T_{sm}$ in units ~!, for an electron confined in boxes with b = 2a, 5a and 10a, in magnetic induction fields defined by the dimensionless magnetic flux parameter $m_e ! b^2 = \sim$.

| | | | | | | | |
|---|---|---|---|---|---|---|---|
| $m_e ! b^2 = \sim$ | | 1 | 1 | 1 | 15 | 15 | 15 |
| $m_e ! a^2 = \sim$ | | 0.25 | 0.04 | 0.01 | 3.75 | 0.6 | 0.15 |
| s | m | $E^T_{sm}$ | $E^T_{sm}$ | $E^T_{sm}$ | $E^T_{sm}$ | $E^T_{sm}$ | $E^T_{sm}$ |
| 1 | 0 | 19.79178 | 7.46920 | 5.65108 | 5.33410 | 2.46994 | 1.91268 |
| | ¨ 1 | 19.72188 | 8.16592 | 6.94048 | 4.40352 | 1.76000 | 1.23668 |
| | | 21.72188 | 10.16592 | 8.94048 | 6.40352 | 3.76000 | 3.23668 |
| | ¨ 2 | 21.50142 | 11.84566 | 11.42684 | 3.61104 | 1.29718 | 1.03460 |
| | | 25.50142 | 15.84566 | 15.42684 | 7.61104 | 5.29718 | 5.03460 |
| | ¨ 3 | 25.09870 | 17.67902 | 17.58700 | 2.95458 | 1.09156 | 1.00632 |
| | | 31.09870 | 23.67902 | 23.58700 | 8.95458 | 7.09156 | 7.00632 |
| | ¨ 4 | 30.46266 | 25.06046 | 25.04484 | | | |
| | | 38.46266 | 33.06046 | 33.04484 | | | |
| | ¨ 5 | 37.52606 | 33.74222 | 33.73996 | | | |
| | | 47.52606 | 43.74222 | 43.73996 | | | |
| 2 | 0 | 79.00098 | 30.51030 | 23.69370 | 9.06064 | 5.06776 | 4.16546 |
| | ¨ 1 | 78.98152 | 31.64624 | 26.04792 | 8.72414 | 4.21142 | 3.41790 |
| | | 80.98152 | 33.64624 | 28.04792 | 10.72414 | 6.21142 | 5.41790 |
| | ¨ 2 | 80.92192 | 36.95496 | 33.94736 | 7.91474 | 3.63896 | 3.11796 |
| | | 84.92192 | 40.95496 | 37.94736 | 11.91474 | 7.63896 | 7.11796 |
| | ¨ 3 | 84.82974 | 45.94932 | 44.86382 | 7.23292 | 3.33512 | 3.09164 |
| | | 90.82974 | 51.94932 | 50.86382 | 13.23292 | 9.33512 | 9.09164 |
| 3 | 0 | 177.69628 | 69.02626 | 54.02880 | 16.23734 | 7.82040 | 6.05602 |
| | ¨ 1 | 177.78674 | 70.32580 | 56.94516 | 15.30200 | 6.95948 | 5.74480 |
| | | 179.78674 | 72.32580 | 58.94516 | 17.30200 | 8.95948 | 7.74480 |
| | ¨ 2 | 179.66006 | 76.24628 | 67.07614 | 14.49612 | 6.38078 | 5.44980 |
| | | 183.66006 | 80.24628 | 71.07614 | 18.49612 | 10.38078 | 9.44980 |
| | ¨ 3 | 183.62184 | 86.71936 | 82.07110 | 13.82010 | 6.09200 | 5.53434 |
| | | 189.62184 | 92.71936 | 88.07110 | 19.82010 | 12.09200 | 11.53434 |

TABLE II. Transverse energy eigenvalues $E^T_{1m}$ as a function of the parameter m + ¹ , Eq. (29), for electron confined in boxes with $m_e\,!\,b^2$=~ = 1 and the indicated values of $m_e\,!\,a^2$=~ and signs of m + ¹ .

| $m_e\,!\,a^2$=~ | 0.25 | | 0.04 | | 0.01 | |
|---|---|---|---|---|---|---|
| m + ¹ | – | + | – | + | – | + |
| jm + ¹j | $E^T_{1m}$ | $E^T_{1m}$ | $E^T_{1m}$ | $E^T_{1m}$ | $E^T_{1m}$ | $E^T_{1m}$ |
| 0 | 19.79178 | 19.79178 | 7.46920 | 7.46920 | 5.65108 | 5.65108 |
| 0.2 | 19.62901 | 20.02901 | 7.33859 | 7.73859 | 5.54960 | 5.94960 |
| 0.4 | 19.54074 | 20.34074 | 7.34598 | 8.14598 | 5.64130 | 6.44130 |
| 0.6 | 19.52680 | 20.72680 | 7.48904 | 8.68904 | 5.91518 | 7.11518 |
| 0.8 | 19.58724 | 21.18724 | 7.76399 | 9.36399 | 6.35476 | 7.95476 |
| 1 | 19.72188 | 21.72188 | 8.16592 | 10.16592 | 6.94048 | 8.94048 |
| 1.2 | 19.93154 | 22.33154 | 8.68844 | 11.08844 | 7.65207 | 10.05207 |
| 1.4 | 20.21310 | 23.01310 | 9.32507 | 12.12507 | 8.47078 | 11.27078 |
| 1.6 | 20.56924 | 23.76924 | 10.06840 | 13.26840 | 9.38064 | 12.58064 |
| 1.8 | 20.99979 | 24.59979 | 10.91102 | 14.51102 | 10.36910 | 13.96910 |
| 2 | 21.50142 | 25.50142 | 11.84566 | 15.84566 | 11.42684 | 15.42684 |
| 2.2 | 22.09683 | 26.49683 | 12.86538 | 17.26538 | 12.54727 | 16.94727 |
| 2.4 | 22.72467 | 27.52467 | 13.96385 | 18.76385 | 13.72597 | 18.52597 |
| 2.6 | 23.44452 | 28.64452 | 15.13541 | 20.33541 | 14.95999 | 20.15999 |
| 2.8 | 24.23603 | 29.83603 | 16.37518 | 21.97518 | 16.24742 | 21.84742 |
| 3 | 25.09870 | 31.09870 | 17.67902 | 23.67902 | 17.58700 | 23.58700 |
| 3.2 | 26.03209 | 32.43209 | 19.04350 | 25.44350 | 18.97790 | 25.37790 |
| 3.4 | 27.03570 | 33.83570 | 20.46588 | 27.26588 | 20.41952 | 27.21952 |
| 3.6 | 28.10905 | 35.30905 | 21.94392 | 29.14392 | 21.91144 | 29.11144 |
| 3.8 | 29.25156 | 36.85156 | 23.47590 | 31.07590 | 23.45330 | 31.05330 |
| 4 | 30.46266 | 38.46266 | 25.06046 | 33.06046 | 25.04484 | 33.04484 |
| 4.2 | 31.74178 | 40.14178 | 26.69655 | 35.09655 | 26.76582 | 35.16582 |
| 4.4 | 33.08831 | 41.88831 | 28.38334 | 37.18334 | 28.37600 | 37.17600 |
| 4.6 | 34.50163 | 43.70163 | 30.12020 | 39.32020 | 30.11521 | 39.31521 |
| 4.8 | 35.98110 | 45.58110 | 31.90662 | 41.50662 | 31.90325 | 41.50325 |
| 5 | 37.52606 | 47.52606 | 33.74222 | 43.74222 | 33.73996 | 43.73996 |

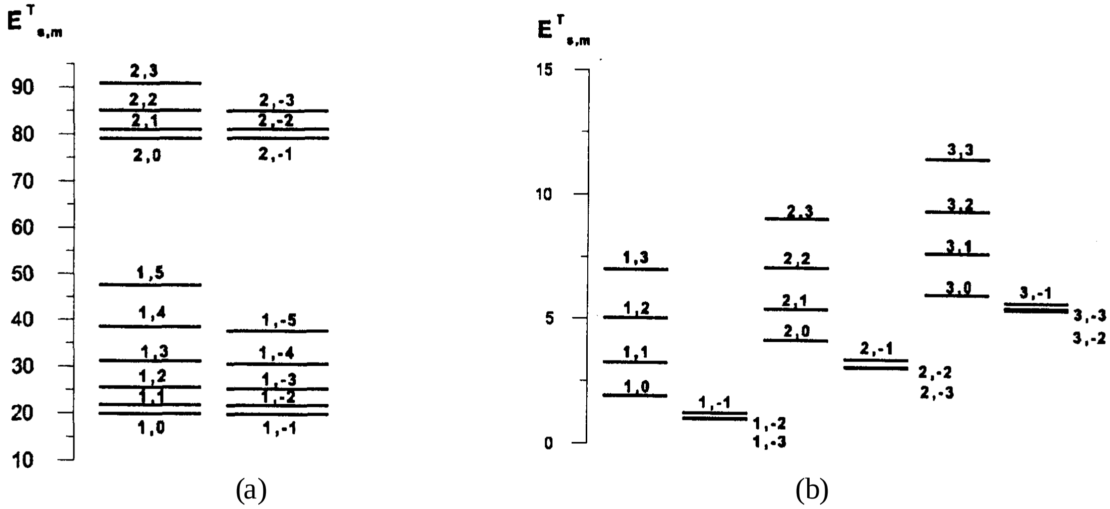


FIG. 1. Lower Landau energy levels $E^T_{sm}$ for an electron confined in boxes with (a) $m_e\omega b^2/\hbar = 1$ and $m_e\omega a^2/\hbar = 0.25$ and (b) $m_e\omega b^2/\hbar = 15$ and $m_e\omega a^2/\hbar = 0.15$.

for the first set of three small boxes and decreases for the set of larger boxes; additionally, within each set, the effect is more noticeable for the boxes with larger perforations.

Figures 1a and 1b illustrate the change of the confinement effect as well as the magnetic field effects in the energy spectra of the electron for the boxes of the first and last columns, respectively. For the small box with $b = 1$ in the unit of length $(\hbar/m_e\omega)^{1/2}$ and large perforation $a = 0.5$, the confinement effect is large as illustrated by numerical values for the eigenergies of the $m = 0$ states in the box expressed in terms of the corresponding normal Landau eigenergies $E^T_{10} = 19.79178E^L_{10}$, $E^T_{20} = 26.33333E^L_{20}$, $E^T_{30} = 35.53925E^L_{30}$, a situation extensive to the other $E^T_{sm}$ states. The reader should notice the different regions in the energy scale in Fig. 1a for the $s = 1$ and 2 energy levels due to the large size of the confinement effect; the inclusion of the $s = 3$ energy levels would require jumping to the region with $E^T_{sm} \geq 170$. The quasi-degeneracy of the energy levels $(s; m \geq 0)$ and $(s; -m-1)$ is readily noticeable, and can be understood as the result of the combination of the confinement effect and the magnetic effects associated with the Landau states, including the distinct behaviour of the $m > 0$ and $m < 0$ states due to the diamagnetic energy. On the other hand, Fig. 1b for a larger box with $b = \sqrt{15}$ and a small perforation $a = \sqrt{15}/10$, the energy scale is the same as for the normal Landau states because the confinement effect is appreciably reduced. Nevertheless it is still definitely present as the comparison $E^T_{10} = 1.91268E^L_{10}$, $E^T_{20} = 1.38849E^L_{20}$, $E^T_{30} = 1.21120E^L_{30}$ indicates. In this case all the energy levels with $s = 1$, 2, and 3 can be drawn together. The spacing of the energy levels for each value of s and the successive positive values of $m$ is not far from 2, the normal Landau energy level spacing. On the other hand, the tendency to degeneracy of the energy levels, for each value of $s$ and the successive negative values of $m = -1; -2; -3; \ldots$, at the normal Landau energy level positions $1; 3; 5; \ldots$ is explicitly apparent. The energy spectra for the electron in the boxes of columns 2-5 in Table I illustrate their intermediate behavior between the two situations explicitly discussed in connection with Figs. 1(a), 1(b).

Table II presents the transverse energy eigenvalues $E^T_{sm}$ for the Landau states with $s$ = 1 and $m$ = 0, $\pm$ 1, $\pm$ 2, $\ldots$ for an electron in boxes with $b$ = 1 and $a$ = 0.5, 0.2 and 0.1, when the magnetic induction fields in the perforation and in the box are different according to Eqs. (26) and (29). The values of $\gamma_s$ are the numerical solutions of Eq. (30) and depend on the value of $|m+\mu|$. The energy eigenvalues themselves also depend on the value and sign of $m+\mu$, as distinguished in the corresponding columns. The first column gives the values of $|m+\mu|$ interpolating between the integer values of $m$ already considered in Table I. Again the values for $\gamma_s$, when doubled and increased by one unit give the entries for the energies in the first, third and fifth columns for the states with $(m+\mu) < 0$, in which the rotational and diamagnetic energies cancel each other (see Eq. (29)). The energies for the following columns are obtained by the further addition of $2|m+\mu|$ and correspond to the states with $(m+\mu) > 0$, Eq. (29).

It is important to understand that the entries in each pair of columns of Table II are valid for the energies $E^T_{sm}(\mu)$ for the different combinations of the values of $m$ of the chosen states, and of the differences $\mu$ of the magnetic induction field in the perforation with respect to the one in the box. For the sake of illustration let us consider the specific value $|m+\mu|$ = 0.2, common to $m+\mu$ = -0.2 and $m+\mu$ = 0.2. The negative value can be obtained from the following combinations $(m;\mu)$ : (0, $-$0.2), ($-$1, 0.8), (1, $-$1.2), ($-$2, 1.8), (2, $-$2.2) $\ldots$; and the positive value from: (0, 0.2), ($-$1, 1.2), (1, $-$0.8), ($-$2, 2.2), (2, $-$1.8), $\ldots$. All of them have the common value of $\gamma_s$ obtained from Eq. (30) with $(m+\mu)$ = 0.2, and, as already stated, the energies for the states with the negative value of $(m+\mu)$ is the entry in the odd column, and the energy for the states with positive values of $(m+\mu)$ is twice this value above. The generalization of this result is

$$E^T_{sm}(m+\mu) = E^T_{s\,m+N}((m+N)+(\mu - N)); \tag{31}$$

with $N = 0; \pm 1; \pm 2; \ldots$ expressing the periodic repetition of the Landau energy levels of the electron in the annular box when the magnetic flux in the perforation changes by one fluxon, accompanied by a compensating shift of one unit in the angular momentum quantum number. This behaviour is graphically illustrated in Figs. 2(a) and 2(b) for the boxes with larger and smaller perforations.

For $\mu = 0$, the energy levels coincide with those of Fig. 1(a) and the third column of Table I. As $\mu$ increases from its initial value, the states with zero and positive values of $m$ increase their energies, while the states with negative values of $m$ decrease their energies; the state $s$ = 1, $m = -1$ energy reaches its minimum value for $\mu \approx 0.5$ in Fig. 2(a) and $\mu \approx 0.8$ in Fig. 2(b). When $\mu$ reaches the value of 1, the first periodic repetition of Eq. (31) with $N$ = 1 is realized, and continues as $\mu$ keeps on increasing. On the other hand, as $\mu$ decreases from zero, the states with zero and positive values of $m$ decrease their energies, and the states with negative values of $\mu$ increase their energies; the state $s$ = 1, $m$ = 0 reaches its minimum value for $\mu \approx -0.5$ in Fig. 2(a) and $\mu \approx -0.2$ in Fig. 2(b). When $\mu$ reaches the value of $-1$, the first periodic repetition of Eq. (31) with $N = -1$ is realized, and continues as $\mu$ keeps on decreasing moving to the left in the graph. By drawing the energy curve $E_{10}(\mu)$ from the data of Table II, the other curves for $E^T_{1m}$ are obtained from horizontal translations of that curve by $m$ units, to the right for negative $m$ and to the left for positive $m$. Here we have illustrated the A-B effect on the Landau states for the energy levels with $s$ = 1, but it holds in general for any $sm$ states, as expressed by Eq. (31).

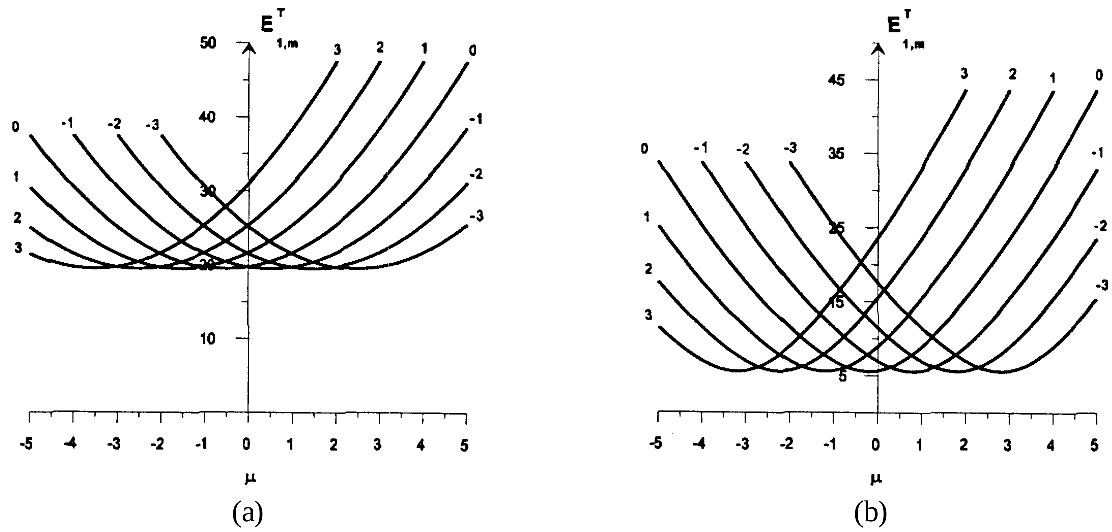


FIG. 2. Aharonov-Bohm effect on Landau energy levels $E^T_{sm}(\Phi)$, as illustrated through their periodic dependence on the change of magnetic flux $\Phi$ in the perforation of annular cylindrical boxes with $m_e\omega b^2/\hbar = 1$, and a) $m\omega_e a^2/\hbar = 0.25$ and b) $m_e\omega a^2/\hbar = 0.01$.

In conclusion, this paper has presented an analysis of the confinement effect in annular cylindrical boxes on the Landau states, and of the A-B effect on such states. The signature of the Landau states in the first system is manifested through the higher energies of the positive m states and lower energies of the negative m states, including the evolution of their degeneracy as the boxes get larger. The A-B effect is manifested through the periodic repetition of the energy spectrum as a function of the variation of the magnetic flux in the perforation of the box with the corresponding shifts in the angular quantum number of the Landau states, and with a period of one fluxon.

## APPENDIX A

The Kummer confluent hypergeometric functions $M$ and $U$ are defined by

$$M(\alpha,\beta,z) = \sum_{s=0}^{\infty} \frac{(\alpha)_s z^s}{(\beta)_s s!} \tag{A.1}$$

in terms of the Pochhammer symbol,

$$(\alpha)_0 = 1, \quad (\alpha)_s = \alpha(\alpha+1)\ldots(\alpha+s-1) = \frac{\Gamma(\alpha+s)}{\Gamma(\alpha)}, \tag{A.2}$$

and

$$U(\alpha,\beta,z) = \frac{\pi}{\sin\pi\beta}\left\{\frac{M(\alpha,\beta,z)}{\Gamma(1+\alpha-\beta)\Gamma(\beta)} - z^{1-\beta}\frac{M(1+\alpha-\beta,2-\beta,z)}{\Gamma(\alpha)\Gamma(2-\beta)}\right\}. \tag{A.3}$$

The series of Eq. (A.1) is convergent for all values of $z$ and all values of $\alpha$ and $\beta$ which are not negative integers. It becomes a polynomial of degree $N$ when $\alpha = -N$ is a negative integer.

When $\beta$ is a positive integer, Eq. (A.3) leads to the logarithmic form

$$
\begin{aligned}
U(\alpha; n+1; z) = \frac{(-)^{n+1}}{n!\,\Gamma(\alpha - n)} \Big[ & M(\alpha; n+1; z) \ln z \\
& + \sum_{r=0}^{\infty} \frac{(\alpha)_r z^r}{(n+1)_r r!} \big\{ \psi(\alpha + r) \\
& - \psi(1+r) - \psi(1+n+r) \big\} \Big] \\
& + \frac{(n-1)!}{\Gamma(\alpha)} z^{-n} M(\alpha - n; 1-n; z)_n ;
\end{aligned}
\tag{A.4}
$$

for $n = 0, 1, 2, \ldots$, where $\psi(x) = \Gamma'(x)/\Gamma(x)$ and the last factor is the sum of $n$ terms with the value zero for $n = 0$. Their asymptotic forms for $z \to \infty$ are

$$
M(\alpha; \beta; z) = \frac{\Gamma(\beta)}{\Gamma(\alpha)} e^z z^{\alpha - \beta} [1 + 0(|z|^{-1})]; \tag{A.5}
$$

$$
U(\alpha; \beta; z) = z^{-\alpha} [1 + 0(|z|^{-1})]. \tag{A.6}
$$

## References


[1] L. D. Landau, Z. Phys. **64**, 629 (1930).

[2] L. D. Landau and I. M. Lifshitz, *Quantum Mechanics*. (Pergamon Press, Oxford, 1977).

[3] M. K. Fung and Y. F. Wang, Chin J. Phys. **37**, 435 (1999).

[4] Y. Aharonov and D. Bohm, Phys. Rev. **115**, 485 (1959).

[5] R. G. Chambers, Phys. Rev. Lett. **5**, 3 (1960).

[6] D. Kouznetsov, E. Ley-Koo and G. Villa-Torres, Rev. Mex. Fís **45**, 485 (1999).

[7] M. Abramowitz and I. Stegun, *Handbook of Mathematical Functions*, (Dover, New York, 1965) Chap. 13.